Structural, Optical and Magnetic Properties of Pristine, (Mn, Al) co-doped ZnO Nanocrystallites Synthesized via co-Precipitation Method

P. Swapna[1], S. Venkatramana Reddy[1,*], B. Sreenivasulu[2]

[1]*Department of Physics, Sri Venkateswara University, Tirupati 517 502, Andhra Pradesh, India*
[2]*Annamacharya Institute of Technology & Sciences, Rajampet 516126, Andhra Pradesh, India*

*Corresponding authors: E-mail: drsvreddy123@gmail.com

Received: 18 March 2019, Revised: 20 June 2019 and Accepted: 25 June 2019

DOI: 10.5185/amlett.2019.0018
www.vbripress.com/aml

Abstract

Undoped and (Mn, Al) co-doped Zinc Oxide nanoparticles are synthesized by chemical co-precipitation method at room temperature effectively via poly ethylene glycol (PEG) as stabilizing agent. XRD data reveals that all the concentrations acquire hexagonal wurtzite crystal structure with no secondary peaks concerning to Al or Mn, indicating successful dissolution of Al and Mn in to ZnO host lattice. The exact particle size is estimated using TEM illustrations, which is confirmed through the XRD results. EDS spectrum shows, no impurities are present in the samples other than manganese and aluminum. The absorption spectra of all the samples reveal characteristic absorption edge in the vicinity of 375 nm. PL spectra show that all the concentrations include defect associated peaks in the visible region. VSM measurements reveal the ferromagnetic nature for co-doped samples. Copyright © VBRI Press.

Keywords: Magnetic studies, defect peaks, Secondary phase, absorption edge and VSM.

Introduction

In recent times dilute magnetic semiconductors (DMSs) had been enticing to an immense extent in view of the fact that they show their feasibility of influencing charge, spin degrees of freedom in a particular substance. By the accumulation of transition material into ZnO, room temperature ferromagnetism (RTFM) in ZnO associated DMS have brought about rigorous attention on ZnO. Due to high solubility of manganese and large band gap of ZnO host lattice, manganese doped ZnO reveals large potential. Furthermore, fascinated much attention for the reason that of disagreements concerning the existence and origin of RTFM [**1**]. Sharma *et al.* [**2**] identified nature of ferromagnetism beyond room temperature in support of small atomic percentages of manganese addition in ZnO bulk and thin films. They projected that RTFM nature appropriate to carrier-induced exchanges between isolated manganese ions in ZnO. But a few authors insisted that RTFM in manganese doped samples emanated from an oxygen vacancy stabilized meta stable phase [**3, 4**]. A few authors showed that the secondary phases of manganese clusters of transition elements and their oxides may be attributable for the identified ferromagnetic nature [**5-7**]. Nevertheless, a few recent analysis revealed that non-appearance of ferromagnetism ordering in bulk single phase of manganese doped Zinc Oxide downward to 2K [**8, 9**]. Similar conflicting consequences have also been identified for manganese doped Zinc Oxide thin films, it broaden from paramagnetic properties [**10**] to spin-glass nature [**11**]. Obviously the variations reported in the literature are owing to diverse synthesizing methods and with several explorations recommending that the magnetic properties are enormously receptive to the synthesized conditions. The aim of the present work is enhancement of luminescence and magnetic properties of the ZnO nanostructures via co-doping with dual impurities. We selected Al and Mn as appropriate dopants for the aim of present study, as Al doped ZnO is considered as a potential tool owing to its remarkable optical transmittance, high conductivity, luminescence, nontoxicity and manganese for its high soluble nature and ferromagnetic behavior at room temperature.

Investigational studies

Preparation of pure and co-doped ZnO nanostructures

Intended for the synthesis of Pristine and (Mn, Al) co-doped Zinc Oxide nanocrystallites, Zinc acetate dehydrate, Potassium hydroxide are used as preliminary materials and manganese acetate tetra hydrate, aluminum nitrate nano hydrate are used for the purpose of doping. All the chemicals are in analytical mark and used with no more purification. To prepare pure Zinc Oxide nanoparticles, Zinc acetate dihydrate solution is mixed with KOH solution with the help of magnetic

stirrer, add 2 ml of PEG to that solution and keep stirring for 10 hrs, white precipitate is formed. For co-doped ZnO nanoparticles add aluminum nitrate nano hydrate and manganese acetate tetra hydrate solutions to the mixed solution of Zinc acetate dehydrate and Potassium hydroxide and add 2 ml of PEG to the solution and keep stirring continuously for 10 hrs, precipitate will form. By filtering the formed precipitate and washed quite a lot of times by means of de-ionized water superfluous elements produced during the progress of preparation are removed. Later all the powders are dried at 70 ^{o}C for 9 hrs and grind the powder samples finely through the aid of agate mortar. Ultimately, all the concentrations are annealed in the furnace at 500 ^{o}C for 1hr.

Characterization techniques of nanosamples

The synthesized samples are cautiously subjected to the subsequent characterizations. Powder X-ray diffraction (XRD) pattern is recorded on Bruker diffracto meter within 2θ range of 20^{o} to 80^{o} via CuKα as X-ray source (λ = 1.53906 Å). Morphological and compositional investigation of pure and co-doped ZnO nanoparticles are deliberated via SEM through EDS (model CARL-ZEISS EVOMA 15). The properties acquired by XRD are corroborated with transmission electron microscopy (TEM) and HRTEM (Model: JEOL JSM 2100). Photoluminescence study is done by PL spectrometer (Model: FLS980 spectrometer) through a 450 W Xenon arc lamp as an excitation source. Magnetic behavior is observed by Vibrating sample magnetometer (VSM).

Results and discussions

Structural properties

XRD Observations

The XRD descriptions of pure and (Mn, Al) co-doped ZnO nanocrystallites are shown in the **Fig. 1**. The peaks of diffraction are resultant to the planes (100), (002), (101), (102), (110), (103) (200), (112), (201) and (202) as well as disclose hexagonal crystalline structure. Also peaks of diffraction relating to pure and doped concentrations correlate to hexagonal wurtzite crystal phase of ZnO and the positions of the diffraction peaks are persistent by the definitive pattern (JCPDS CARD NO:36-1451). Non-existence of secondary peaks denotes absence of impurity phases relating to aluminum or manganese in reach the detection range of the apparatus. The peaks connecting to (Mn, Al) co-doped Zinc Oxide nanoparticles shows high intensity considering with the pure Zinc Oxide nanoparticles, by this we can estimate that by adding manganese in the enhanced concentration into ZnO, the diffracted peak intensity is obtainable high. Furthermore, by the enhancement of the manganese concentration into ZnO, the diffraction peaks shifted towards higher wavelength. The nanoparticle size is estimated by the Debye-scherer formula d = 0.91λ/β cosθ, where'd' is the nanoparticle size, 'λ' is the wavelength of the X-rays and 'θ' is the Bragg's angle of diffracted rays. The calculated particle size of pristine and (Mn, Al) co-doped ZnO are in the range of 21 and 18 nm respectively. By the estimated values of diffraction peaks, we recognized that the crystallite size diminishing with the enhanced manganese concentration. From this it is distinguished that XRD pattern of co-doped ZnO nanocrystallites have huge crystalline character considering by means of pure ZnO.

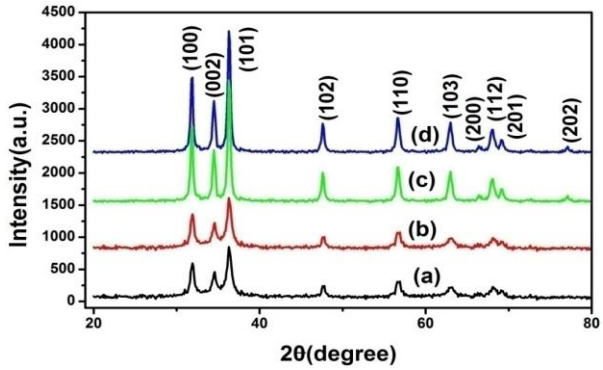

Fig. 1. XRD picture of (a) Pristine ZnO (b) 1 mol% (c) 2 mol% (d) 3 mol% of manganese co-doped with 5 mol % of aluminum (Al as constant at 5 mol %) Zinc Oxide nanoparticles.

Raman spectroscopy observations

For determining the incorporation of dopants, defects and also lattice disorder in a host lattice, Raman spectroscopy is a significant technique [**12**]. **Fig. 2** shows the Raman spectra of pristine and (Mn, Al) co doped Zinc Oxide nanoparticles, Raman spectra of pristine and (Mn, Al) co-doped ZnO shows the peaks at 158 cm^{-1}, 580 cm^{-1} which are endorsed to 1st and 2nd order vibration modes of Zinc Oxide nanoparticles [**13**]. The Raman intensive peak observed at 436 cm^{-1} attributed to mode of higher frequency (E_{2H}). Additional peaks identified at 330 cm^{-1} and 831 cm^{-1} might attributed to multi phonon modes E_{2H}-E_{2L} and (A1(TO)+E_{2L}) correspondingly. One more peak found at 881 cm^{-1} ascribed to Zn-O-Zn vibration mode [**14**]. Together the spectra of pristine and doped ZnO samples include all the most important peaks which are feature modes in ZnO are present in all the samples.

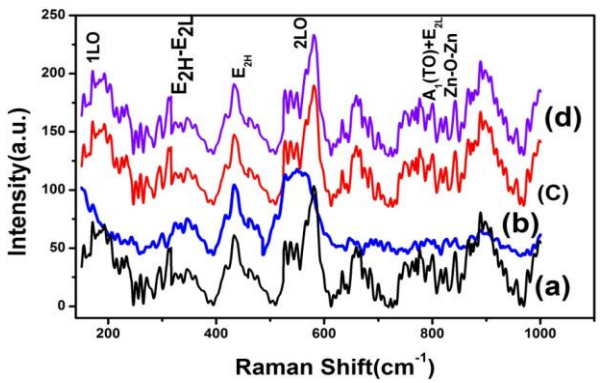

Fig. 2. Raman spectra of (a) Pure ZnO (b) 1 mol% (c) 2 mol% (d) 3 mol% of manganese co-doped with 5 mol% of aluminum (Al as 5 mol % at constant) ZnO nanoparticles.

Morphological and elemental observations

SEM and EDAX observations

Scanning electron microscopy (SEM) is used to estimate the morphological nature of pure and (Mn, Al) doped Zinc Oxide nanocrystallites. The images of the pure Zinc Oxide nanocrystallites show less agglomeration where as co-doped concentrations show high agglomeration with increasing the manganese concentration (**Fig. 3**). All the descriptions are plainly representing the non-homogeneous spherical and irregular nature of the nanocrystallites. EDS spectrum (**Fig. 4**) indicate the incorporation of dopants into ZnO host lattice, this clearly shows the presence of impurity elements such as manganese and aluminum also revealing absence of other impurities in ZnO. The EDS spectrum of pure ZnO shows only Zn and O elements. Weight and atomic percent of Zn, O, Mn and Al are presented in **Table 1**.

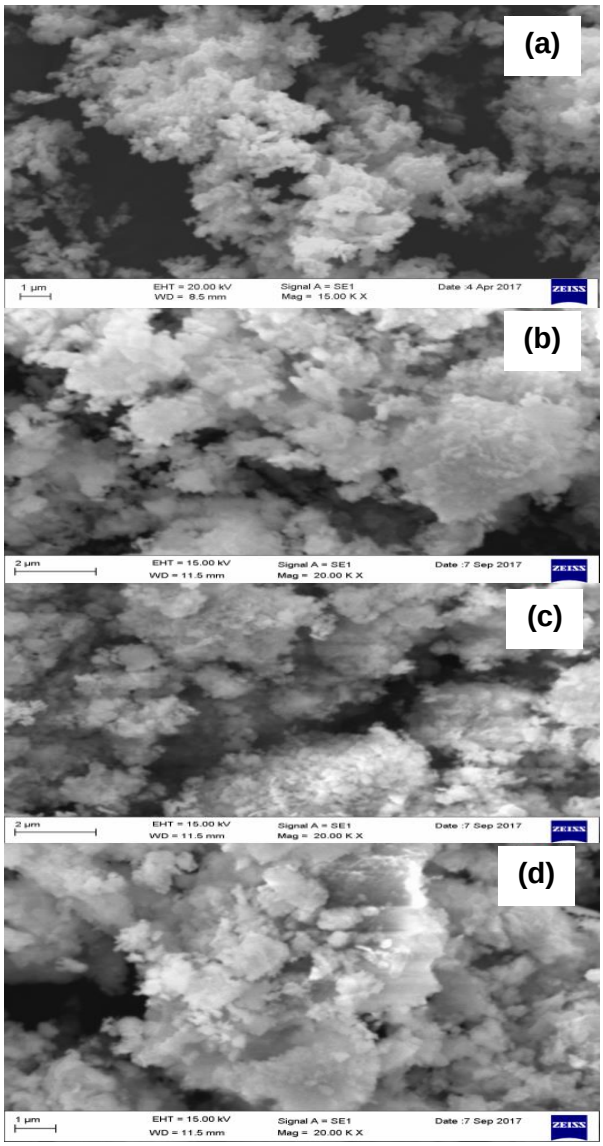

Fig. 3. SEM illustrations of (a) Pristine ZnO (b) 1 mol% (c) 2 mol% (d) 3 mol% of Mn co-doped with Al (Al as 5 mol % at constant) Zinc Oxide nanoparticles.

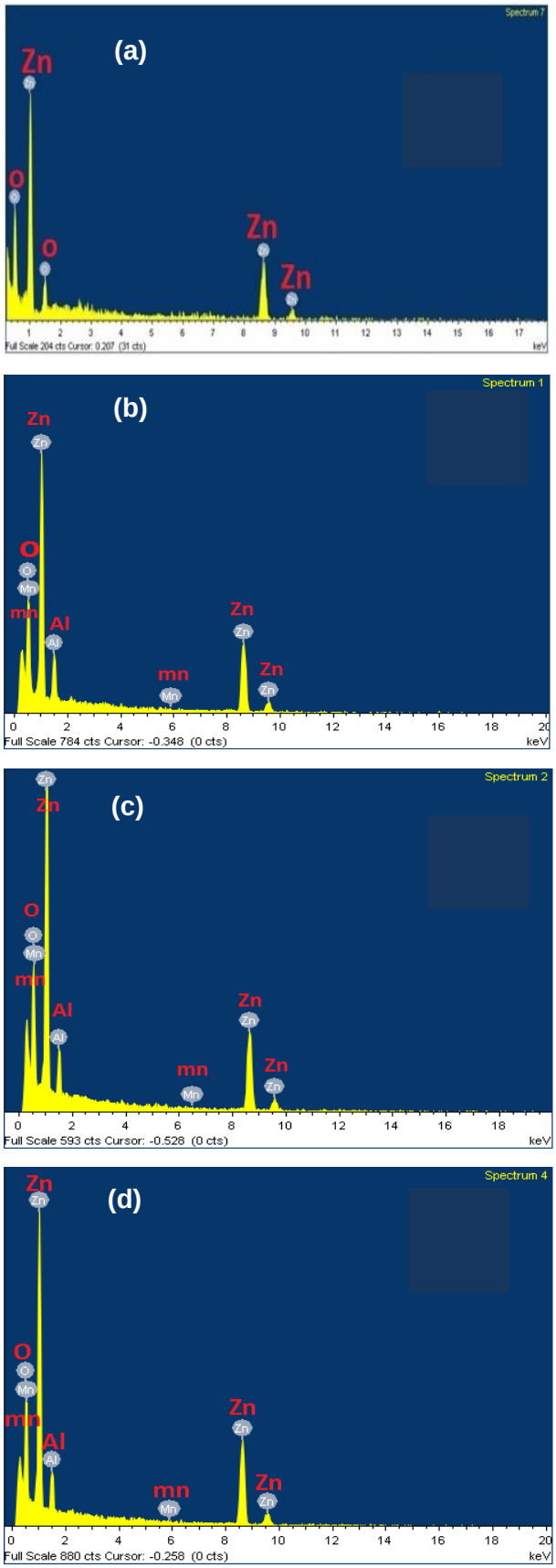

Fig. 4. EDS spectrum of (a) pristine ZnO (b) 1 mol% (c) 2 mol% (d) 3 mol% of Mn co-doped with Al (Al as 5 mol % at constant) Zinc Oxide nanoparticles.

Table 1. The weight and atomic percent of Zn, O, Mn and Al.

Sample	Zinc		Oxygen		Manganese		Aluminum	
	Weight %	Atomic %	Weight %	Atomic %	Weight%	Atomic %	Weight %	Atomic %
Pristine ZnO	59.88	26.76	40.12	73.24	-	-	-	-
Mn-1, Al-5 mol%	63.19	31.77	28.08	57.67	0.11	0.07	8.62	10.49
Mn-2, Al-5 mol%	61.87	30.35	29.99	60.10	0.21	0.12	7.93	9.43
Mn-3, Al-5 mol%	65.75	34.24	26.19	55.72	0.19	0.12	7.87	9.92

TEM, HRTEM and SAED analysis

TEM is undertaken to estimate the accurate size of the pure and co-doped Zinc Oxide nanocrystallites. **Fig. 5** shows the images of pristine and (Mn, Al) co-doped Zinc Oxide nanoparticles. The particle sizes predictable with TEM pictures are approximately confirmed by the XRD data. **Fig. 6** shows the HRTEM illustrations and SAED pattern of pure and co-doped Zinc Oxide nanoparticles. HRTEM descriptions of the pure ZnO show the 5 nm lattice fringes whereas (Mn, Al) co-doped samples show 2 nm lattice fringes. In the HRTEM images, expected d-spacing values of pure and (Mn, Al) co-doped Zinc Oxide nanocrystallites between two nearby lattice fringes are identified as 0.28 nm, 0.26 nm correspondingly and in consequence, it consistent to (101) planes of hexagonal wurtzite crystal structure of ZnO nanocrystallites. SAED pattern of pristine and (Mn, Al) co-doped Zinc Oxide nanocrystallites clearly shows the spotted diffraction in ring pattern in addition at random positions. It shows that pure and doped Zinc Oxide nanocrystallites are single and poly-crystalline in nature. The expected spots of diffraction and rings are indexed through the aid of bulk ZnO data (JCPDS card NO: 36-1451). SAED pattern of pristine and doped Zinc Oxide nanocrystallites are consistent with the XRD data.

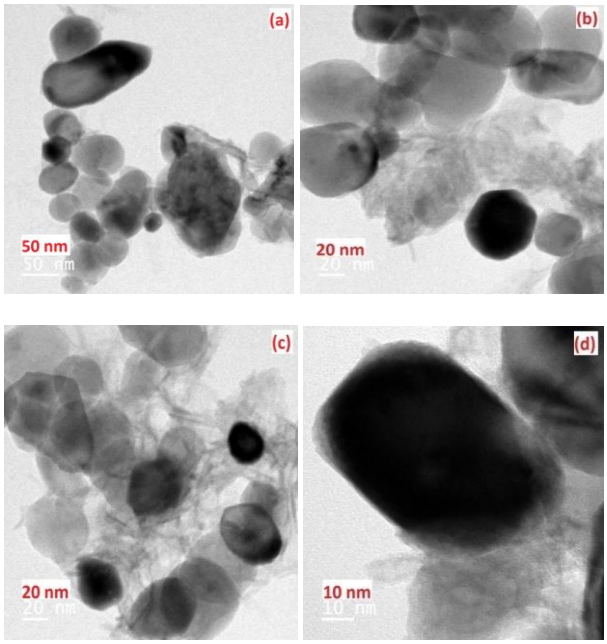

Fig. 5. TEM images of (a) Undoped ZnO (b) 1 mol% (c) 2 mol% (d) 3 mol% of Mn co-doped with aluminum (Al as 5 mol % at constant) Zinc Oxide nanoparticles.

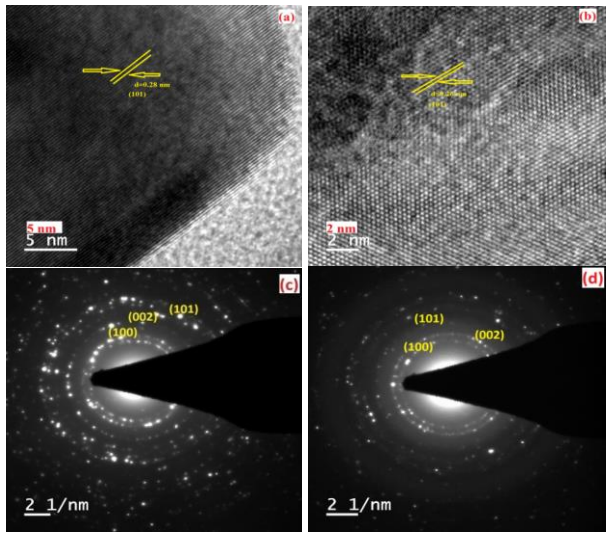

Fig. 6. HRTEM illustrations of (a) Undoped ZnO (b) 3 mol% of Mn doped ZnO nanoparticles (by keeping 'Al' 5.0 mol% as constant). SAED pattern of (c) Undoped ZnO (d) 3 mol% of Mn doped Zinc Oxide nanoparticles (by keeping 'Al' 5.0 mol% as constant).

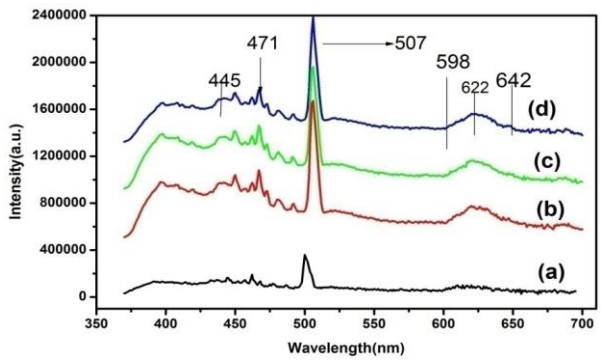

Fig. 7. Photoluminescence spectra of (a) pure ZnO (b) 1 mol% (c) 2 mol% (d) 3 mol% of Mn co-doped with 5 mol % of aluminum Zinc Oxide nanoparticles.

Optical studies

Photoluminescence (PL) Analysis

Photo luminescence spectroscopy (PL) is taken to study the emission nature of pristine and (Mn, Al) co-doped samples, recorded at room temperature in the ambit of 300 nm to 700 nm (**Fig. 7**). Found all the emission peaks in the visible region and the peaks are at 421 nm, 445 nm, 450 nm, 471 nm, 507 nm, 605 nm etc., the peaks originated at 421 nm and 445 nm attributed to defects such as Zinc vacancies (Vzn), Oxygen vacancies (Vo), and interstitials (Zni) correspondingly [**15-18**]. The blue emission peaks are observed at 446 nm, 450 nm, and 471 nm, origin of blue emission is

ascribed to oxygen vacancies (Vo) as studied by R. Wu *et al.* and M. Ghosh *et al.* [**19, 20**]. The green emission peak appeared at 507 nm might be attributed to the impurity levels be compatible with single ionized oxygen vacancy in ZnO nanostructures [**21-23**]. Broad emission band appeared in orange and red region from 598 nm to 642 nm centered at 622 nm, the peaks found in the visible range might be attributed to origin of defects such as oxygen vacancies (Vo) and intrinsic defects (Zni) in Zinc Oxide nanocrystallites as reported by R. Elilarassi *et al.* [**22**].

UV-Vis-NIR studies

Absorption spectra analysis

The absorption spectra of pristine and (Mn, Al) co-doped Zinc Oxide nanoparticles is shown in the **Fig. 8**. Absorption spectroscopy is an important and potential technique to study the optical nature of semiconducting nanostructures [**18**]. UV-Vis-NIR spectroscopic analysis is done at room temperature to look into doping influence of manganese on band gap in the limit of 200 nm to 900 nm. In the wavelength range of 200-380 nm, all the absorption curves demonstrate an intensive absorption through the absorption edge connecting 320 and 380 nm, due to comparatively great exciton binding energy, the results are agreed fine with those obtained by earlier reports [**24, 25**]. The absorption spectra of all the samples reveal characteristic absorption edge in the vicinity of 375 nm. The absorbance's of the peaks decline and the positions of the peaks shifting towards lesser wavelength side by enhancing manganese dopant concentration into ZnO, which is obvious in **Fig. 8**, this reveals that the band gap of ZnO increases by the enhancement of Mn^{2+} dopant element concentration into host lattice. The blue shift or enhance in the band gap energy might be explained with the Quantum confinement effect [**26, 27**].

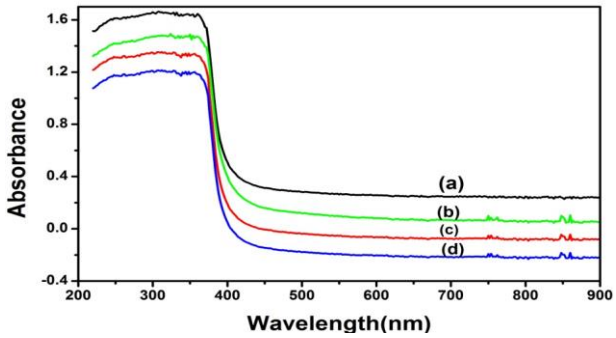

Fig. 8. Optical absorption spectra of (a) Undoped ZnO (b) 1 mol% (c) 2 mol% (d) 3 mol% of Mn co-doped with 5 mol % of aluminum ZnO nanoparticles.

The optical transmittance of pristine and (Mn, Al) doped ZnO nanocrystallites in the wavelength range of 200 nm to 900 nm with varying the concentration of manganese from 1 mol % to 3 mol % (Al at 5 mol% as constant) is shown in **Fig. 9**.

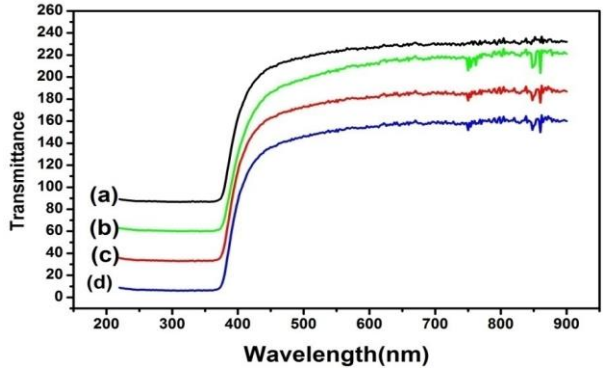

Fig. 9. Optical transmittance of (a) Undoped ZnO (b) 1 mol % (c) 2 mol % (d) 3 mol % of Mn co-doped with 5 mol % of aluminum Zinc Oxide nanoparticles.

Magnetic properties

Magnetization curves of (Mn, Al) co-doped Zinc Oxide nanocrystallites at room temperature are shown in the figure 10. Pristine ZnO reveals diamagnetic behavior as we not shown in the graph, this is recognizable that pure bulk ZnO reveals diamagnetism nevertheless recent reports revealed that pure ZnO can display ferromagnetism below of certain film thickness [**28**], a few authors also reported room temperature ferromagnetism (RTFM) in pristine ZnO [**29, 30**]. This might be ascribed to vacancy related defects which could induce a magnetic moment in the insulator, here in the present work co-doped ZnO samples keeping Al is constant at 5 mol % and changing the concentrations of manganese from 1 mol % to 3 mol % shows the ferromagnetic nature. With increasing the concentration of manganese from 1 to 3 mol % the Saturation Magnetization (Ms) and Retentivity (Mr) values increases and Coercitivity (Hc) values decreases for 2 mol % and increases for 3 mol %. Ms, Mr and Hc values of all the three co-doping concentrations of manganese (keeping Al at constant 5 mol %) are provided in the **Table 2**. **Fig. 11** illustrates the room temperature M-H curves of enlarged lower field region of **Fig. 10**.

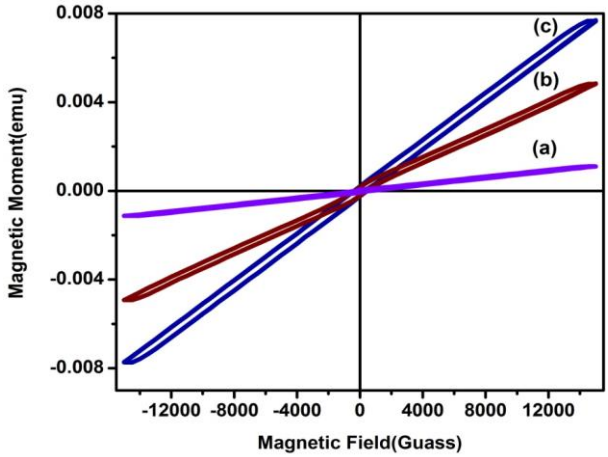

Fig. 10. RT M-H curves of (a) 1 mol % (b) 2 mol % (c) 3 mol % of Mn co-doped with 5 mol % of aluminum Zinc Oxide nanoparticles.

Table 2. Coercivity (Hc), Retentivity (Mr) and Saturation magnetization (Ms) values for (Mn, Al) co-doped ZnO Nano crystallites.

Sample	Magnetization (Ms) (emu/g)	Coercitivity (Hc) (Kilo Guass)	Retentivity (Mr) (emu/g)
Mn-1mol % , Al-5mol %	0.015	0.466	0.0006
Mn-2mol %, Al-5 mol %	0.152	0.395	0.0060
Mn-3mol %, Al-5 mol %	0.241	0.399	0.0065

Fig. 11 shows room temperature (RT) M-H curves of co-doped Zinc Oxide nanocrystallites in the lower field region which is expanded. 3 mol % of Mn shows highest Ms and Mr values compared to left over concentrations.

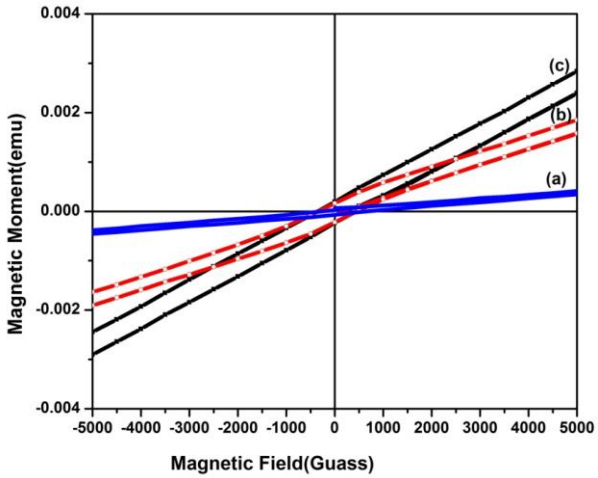

Fig. 11. RT M-H curves of enlarged lower field range of (a) 1 mol % (b) 2 mol % (c) 3 mol % of Mn co-doped with 5 mol % of aluminum Zinc Oxide nanoparticles.

Conclusions

Pure and (Mn, Al) co-doped ZnO nanoparticles are synthesized productively by means of chemical co-precipitation method using PEG as stabilising agent at room temperature. The prepared samples are characterized through XRD, SEM with EDS, TEM, HRTEM, SAED pattern, PL, UV-Vis-NIR and VSM techniques and deliberated diverse kind of properties such as structural, morphological, compositional, optical and magnetic. EDS and TEM analysis is reliable with XRD data. XRD data reveals that all the concentrations possess hexagonal wurtzite crystal structure, TEM images demonstrate the accurate size of the crystallite, which is approximately consistent with XRD, UV-Vis-NIR study reveals the absorption in the region of 200 nm to 380 nm, photoluminescence spectrum reveals the emission peaks relating to defects and VSM measurements display the ferromagnetic nature of the co-doped concentrations.

Conflict of interests

The authors affirmed that there is no conflict of interests concerning the publication of this paper.

Acknowledgements

One of the authors thankful to the University Grants Commission (UGC), New Delhi, India for giving financial assistance by RFSMS program and also thankful to IIT Bombay (SAIF) for making TEM characterization.

References

1. Djaja, N. F.; Saleh, R.; *Materials Sciences and Applications*, **2012**, *3*, 245.
2. Sharma, P.; Gupta, A.; Rao, K. V. ; Owens, F. J. ; Sharma, R.; Ahuja, R.; Osorio, J. M. ; Johansson, B.; Gehring, G. A.; *Nature Matter*, **2003,** *2*, 673.
3. Kundaliya, D.C.; Ogale, S.B.; Lofland, S.E.; Dhar, S.; Metting, C.J.; Shinde, S.R.; Ma, Z.; Varughese, B.; Ramanujachari, K.V.; Salamanca-Riba, L.; Venkatesan, T.; *Nature Matter*, **2004**, *3*, 709.
4. Li, J. H.; Shen, D. Z.; Zhang, J. Y.; Zhao, D. X.; Li, B. S.; Lu, Y. M.; Liu, Y. C.; Fan, X. W.; *Journal of Magnetism and Magnetic Materials*, **2006**, 302, 118.
5. Banerjee, S.; Rajendran, K.; Gayathri, N.; Sardar, M.; Senthilkumar, S.; Sengodan, V.; *Journal of Applied Physics* **2008**, *104*, 043913.
6. Thota, S.; Dutta, T.; Kumar, J.; *Journal of Physics: Condensed Matter*, **2006,** 18, 2473.
7. Park, J. H.; Kim, M. G.; Jang, H. M.; Ryu, S.; Kim, Y. M.; *Applied Physics Letters*, **2004**, *84*, 1338.
8. Lawes, G.; Risbud, A.S.; Ramirez, A. P.; Seshadri, R.; *Physical Review B*, **2005**, *71*, 045201.
9. Rao, C.N.R.; Deepak, F.L.; *Journal of Materials Chemistry*, **2005**, *15*, 573.
10. Tiwari, A.; Jin, C.; Kvit, A.; Kumar, D.; Muth, J. F.; Narayan, J.; *Solid State Communications*, **2002**, *121*, 371.
11. Fukumura, T.; Jin, Z.W.; Kawasaki, M.; Shono, T.; Hasegawa, T.; Koshihara, S.; Koinuma, H.; *Applied Physics Letters*, **2001**, *78*, 958.
12. Singhal, A.; Achary, S.N.; Manjanna, J.; Chatterjee, S.; Ayyub, P.; Tyagi, A.K.; *J. Phys. Chem. C*, **2010**, *114*, 3422.
13. Che, P.; Liu, W. B.; Guo, L.; He, L.; Chen, C. P.; *J. Magn. Magn. Mater.*, **2008**, *320*, 2563.
14. Sankara Reddy, B.; Venkatramana Reddy, S.; Koteeswara Reddy, N.; *J. Mater. Sci.: Mater Electron*, **2013**, *24*, 5204.
15. Udayakumar, S.; Renuka, V.; Kavitha, K.; *J. Chem. Pharm. Res.*, **2012**, *4*, 1271.
16. Qiu, Y.C.; Chen, W.; Yang, S.H.; Zhang, B.; Zhang, X.X.; Zhong, Y.C.; Wong, K.S.; *Cryst. Growth Des,*. **2010**, *10*, 177.
17. Aneesh, P.M.; Cherian, C.T.; Jayaraj, M.K.; Endo, T.; *JCS Japan*, **2010**, *118*, 333.
18. Swapna, P.; Venkatramana Reddy, S.; *IOP Conf. Series: Materials Science and Engineering*, **2018**, *310*, 012011.
19. Wu, R.; Yang, Y.; Cong, S.; Wu, Z.; Xie, C.; Usui, H.; Kawaguchi, K.; Koshizaki, N.; *Chem. Phys. Lett.*, **2005**, *406*, 457.
20. Ghosh, M.; Raychaudhuri, A.K.; *Nanotechnology*, **2008**, *19*, 445704.
21. Swapna, P.; Venkatramana Reddy, S.; *Mechanics, Materials Science & Engineering*, **2017**.
22. Elilarassi, R.; Chandrasekaran, G.; *J Mater Sci: Mater. Electron*, **2010**, *21*, 1168.
23. Muthukumaran, S.; Gopalakrishnan, R.; *Optical Materials*, **2012**, *34*, 1735.
24. Senthilkumaar, S.; Rajendran, K.; Banerjee, S.; Chini, T.K.; Sengodan, V.; *J. Mater. Sci. Semicond. Process.*, **2008**, *11*, 6.
25. Omri, K.; El Ghoul, J.; Lemine, O.M.; Bououdina, M.; Zhang, B.; El Mir, L.; *Superlattices & Microstructures*, **2013**, *60*, 139.
26. Singla, M.L.; Shafeeq, M.M.; Kuma, M.; *J. Lumin.*, **2009**, *124*, 349.
27. Bhargava, R.N.; Gallagher, D.; *Phys. Rev. Lett.*, **1994**, *72*, 416.
28. Kapilashrami, M.; Xu, J.; Rao, K.V.; Belova, L.; *Processing and Application of Ceramics*, **2010**, *4*, 225.
29. Hu, J.; Zhang, Z.; Zho, Z.; Qin, H.; Jiang, M.; *Appl. Phys. Lett.*, **2008**, *93*, 192503.
30. Kapilashrami, M.; Xu, J.; Ström, V.; Rao, K.V.; Belova, L.; *Appl. Phys. Lett.*, **2009**, *95*, 033104.

